THE BELL SYSTEM TECHNICAL JOURNAL
Vol. 52, No. 4, April, 1973
Printed in U.S.A.

Prefilters, Sampling, and Transmission Rates for Intraframe Codecs for *Picturephone*® Service

By R. T. BOBILIN

(Manuscript received September 21, 1972)

This study of prefilters and sampling rates analyzes the edge busyness phenomenon which is a very significant degradation introduced by intraframe video coders. For any given transmission rate, the prefilter and sampling rate can be varied to yield a tradeoff between the edge busyness and the rise time associated with a video transition. A narrower prefilter results in less edge busyness but slower rise times and vice versa. Similarly, varying the sampling rate implies an inverse variation in the number of bits per sample allowed in the quantizer, which leads to a tradeoff between aliasing and quantizing noise, both of which are components of the edge busyness phenomenon. This paper shows in detail how the prefilter, sampler, and quantizer affect both edge busyness and rise time, and optimizes the intraframe coder design as a function of transmission rate from an analysis of this two-factor tradeoff.

I. INTRODUCTION

The goal of this paper is to study the effects of filtering and sampling in the digital processing of signals for *Picturephone*® service. In doing this we are ultimately interested in choosing the optimum prefilters and sampling rates (and therefore the number of bits per sample used in the quantizer) for intraframe DPCM codecs. To simplify the analysis it is assumed that the edge busyness phenomenon is the most significant degradation introduced by these codecs. It will be shown how this edge busyness is affected by each part of the codec and how it can be controlled by trading it off against picture resolution. The main theme of this study is this tradeoff between the detrimental effects of both edge busyness and degraded rise times. Both factors are associ-

ated with video edges and hence only edges, modeled as step functions, will be considered.

Section II is a brief description of the analog *Picturephone* system, which outlines relevant short-haul system specifications. Section III defines edge busyness and shows why it is such a significant video impairment; it also describes how edge busyness is affected by each part of the codec and how it can be controlled by trading it against picture resolution. This edge busyness—resolution tradeoff is further investigated in Section IV which uses a series of subjective pair comparison tests to determine the optimum tradeoff as a function of system quality. Section V uses the results of Sections III and IV to show that optimum coder composition, in terms of prefiltering, sampling rate, and quantizer structure, is a function of the digital transmission rate. This study is concluded in Section VI with a subjective testing program which substantiates the validity of the edge busyness—rise time evaluation of video coders and rates a number of intraframe coders on a five-comment impairment scale.

II. ANALOG SYSTEM DESCRIPTION

For the purposes of this study, the important parts of the analog *Picturephone* system can be modeled as illustrated in Fig. 1. Here both the camera system and all analog links connecting the transmitter to the receiver are nominally flat to 1 MHz. If all the frequency shaping in the receiver (excluding de-emphasis) is combined into one equivalent rolloff filter, the resulting filter has a crispened Gaussian response that rolls off to -20 dB at 1 MHz. Hence the total optics-to-optics step response of the analog *Picturephone* system is dominated by that of the receiver station set.* This total optics-to-optics rolloff and overshoot characteristic is given by:†

$$|R(f)|^2 = \{[1 + K(f/T)^2] \exp [-0.5(f/T)^2]\}^2 \tag{1}$$

where f is in MHz and:

$$K = 0.5292$$
$$T = 0.35592.$$

From this the step response can be shown to be (assuming linear phase with a slope of t_0):

$$s(t) = \tfrac{1}{2} \operatorname{Erf}(B) + \frac{BK}{\sqrt{\pi}} \exp(-B^2) \tag{2}$$

* See Ref. 1, pp. 291–292.
† See Ref. 2, eq. (8), but add a set of missing parentheses.

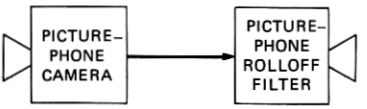

Fig. 1—Analog system model.

where

$$B = \sqrt{2}\pi T(t - t_0) \times 10^6.$$

This step response is plotted in Fig. 2. The response is symmetric about the half-amplitude point with a 4-percent single undershoot and overshoot and has a 10- to 90-percent rise time (T_R) of 0.69 μs.

III. DIGITAL SYSTEM DESCRIPTION

The essential parts of the intraframe DPCM digital system model are illustrated in Fig. 3. In addition to the analog system already described, there is a prefilter, and there are sampling circuits and a quantizer-decoder combination. The prefilter limits line interference and shapes the analog video signal to be encoded. The sample-and-hold and sampling clock circuits turn the analog video into a discrete time format. The quantizer is used to classify the sample-and-hold outputs into a finite number of values for transmission over a given digital channel. The decoder is the inverse of the DPCM quantizing algorithm and

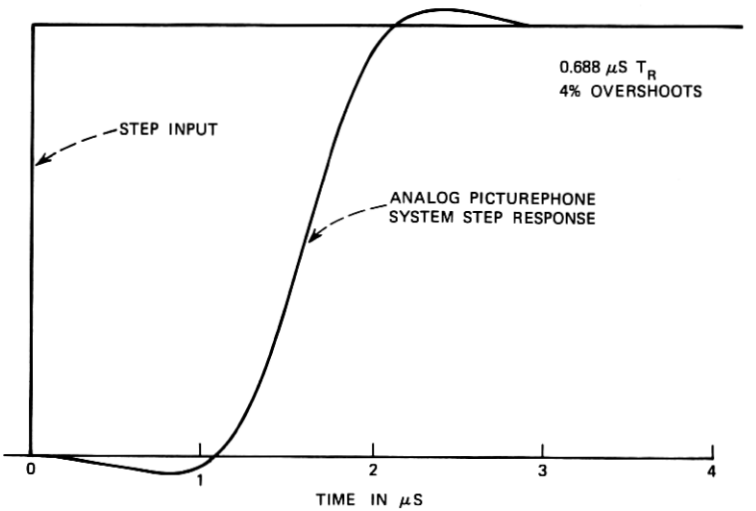

Fig. 2—Analog system step response.

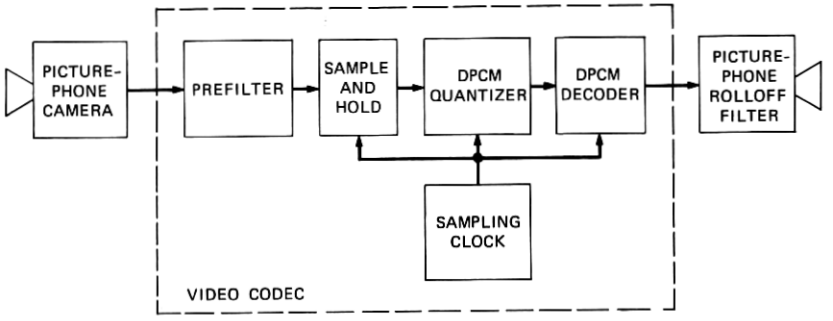

Fig. 3—Digital system model.

puts out the quantized version of the coder's sample-and-hold waveform to the receiving analog system.

In order to see what the codec does to a video transition (such as the edge of a face or a shirt or any black-white boundary), let us start with the simplest part of the codec and study its effect on the video signal. Then the remaining parts of the codec can be added one at a time and analyzed. All step responses will be measured at the output of the analog receiver, as would be seen by the user.

3.1 *Sampling Circuits*

Consider the simplest video codec consisting of only a sample-and-hold circuit driven by a sampling clock. Hence the prefilter, quantizer, and decoder circuits of Fig. 3 are deleted. If we model the ouput of the *Picturephone* transmitter as a perfect step function (the validity of this model will be discussed in the next section), the input to the codec sample-and-hold circuit is illustrated in Fig. 4a. If the sampling instants of the coder clock are given by sampling Phase 1 in Fig. 4a, then the outputs of the sample-and-hold circuit and the receiver rolloff filter are those designated Phase 1 in Figs. 4b and 4c, respectively. If the phasing of the sampling clock with respect to the step function was changed by a quarter of the sampling period, the sampling instants could be given by sampling Phase 2 of Fig. 4a. The resulting outputs of the sample-and-hold circuit and the receiver rolloff filter would be given by the Phase 2 curves in Figs. 4b and 4c, respectively. The outputs from this second phasing of the sampling clock would be the same as those of the first phasing delayed by $T/4$. If the sampling clock were delayed as given by sampling Phase 3 and 4, the corresponding outputs would be given by the Phase 3 and 4 waveforms in Figs. 4b and 4c, respectively.

In this way we can see that the step response of this digital system (always observed at the output of the receiver rolloff filter) will always have the same shape as that of the analog system. The time of occurrence of the step response will depend on the relative phasing of the sampling clock with respect to the camera step function. This indeterminacy of the edge location due to the sampling phase dependence is one specific example of aliasing and will henceforth be called sampling-induced busyness (SIB). Quantitatively, this sampling-induced busyness will be measured as the maximum indeterminacy of the edge at the 50-percent amplitude point. This measure is illustrated in Fig. 4c and in this case is equal to T, one sampling interval.

Sampling-induced busyness is detrimental because it causes the

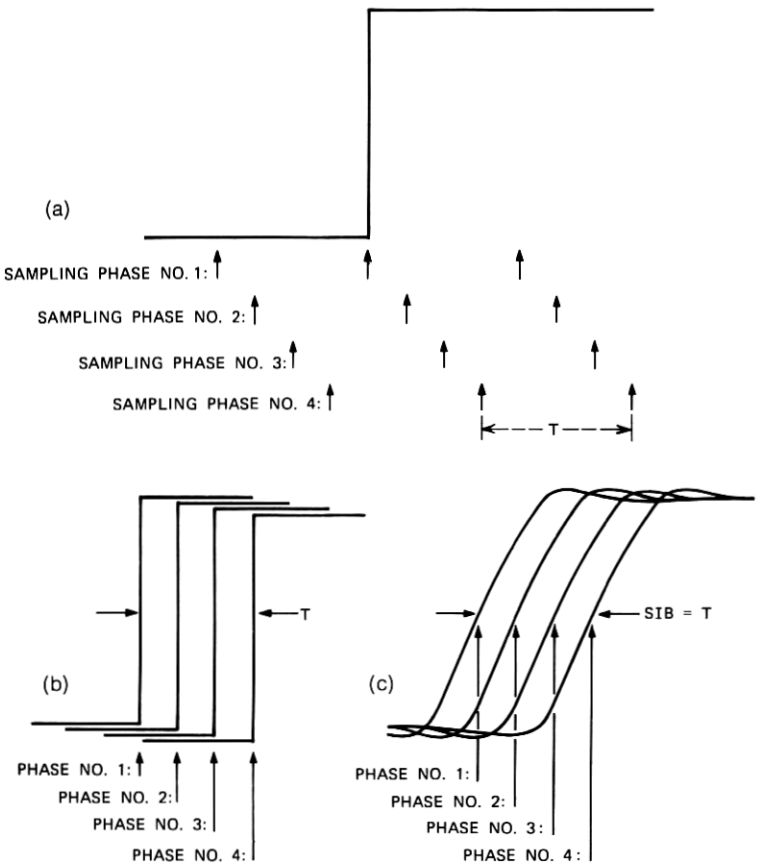

Fig. 4—(a) Step input from camera. (b) Decoder output. (c) Rolloff filter output.

breakup of edges and is easily seen in a typical *Picturephone* display. To see how this breakup occurs, turn to Fig. 5. This represents an enlargement of a small section of a *Picturephone* display. Only five (L1 to L5) of the 267 lines in a frame are illustrated, and only four sampling instants (S1 to S4) are shown. The main diagonal represents the edge of a black-white transition. In the original scene all the area to the left of the edge is black and all area to the right of the edge is white. On line L1, the black-white transition is detected by the sampler at sampling instant S4. On line L2, the transition is also detected at sampling instant S4. It is detected at S3 on line L3 and at S2 on both lines L4 and L5. Thus the transition is detected at the times indicated by circles on Fig. 5. After these sample-and-hold waveforms are passed through the receiver rolloff filter, the edge of the black-white transition would appear to the observer to be the crooked dashed curve of Fig. 5.

For a codec whose sampling clock is locked to the raster, the above curvature is motionless if the edge is still. If the codec is not locked to the raster or if the edge is moving from frame to frame, the above curvature will crawl through the picture. A straight line will be

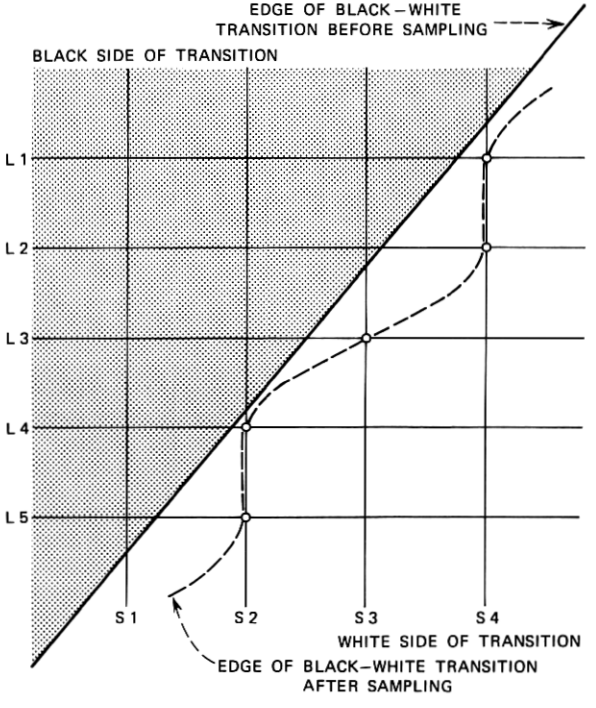

Fig. 5—Sampling-induced busyness.

turned into a moving crooked edge. This effect is extremely visible and quite annoying for an unfiltered sampled-and-held picture.

The only effect of introducing the sampling circuits into the analog system is this edge indeterminance we have called sampling-induced busyness. The rise time of the system has not been affected by the sampling circuits.

3.2 *Prefilter*

The addition of the prefilter changes the input to the sample-and-hold circuit from a perfect step function to a gentler transition with a nonzero 10- to 90-percent rise time as might be given in Fig. 6a. The

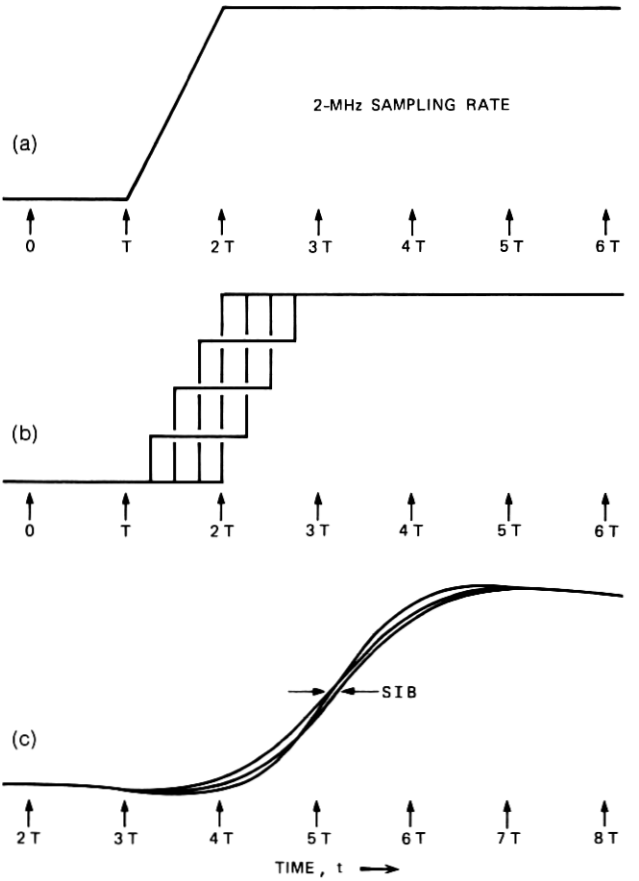

Fig. 6—Effect of prefilter on SIB. (a) Prefilter output. (b) Sample-and-hold output. (c) *Picturephone*® receiver output.

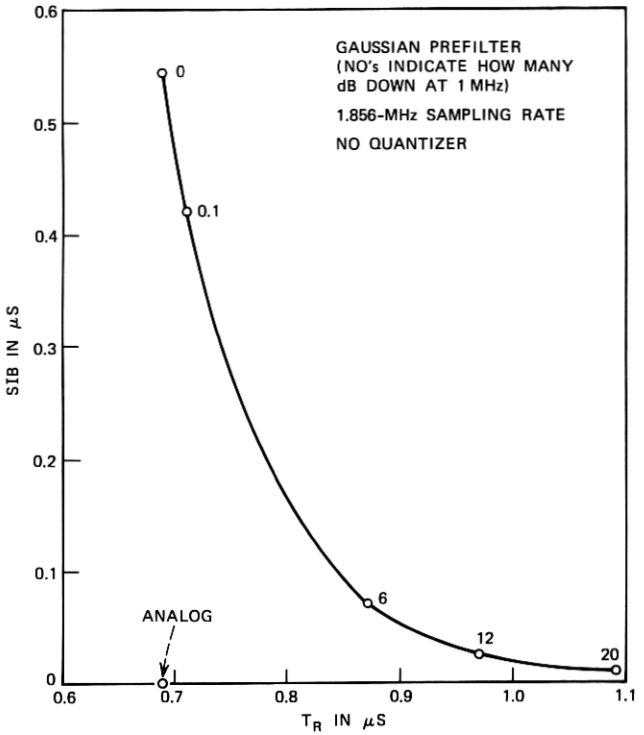

Fig. 7—Sampling-induced busyness—rise time tradeoff.

more prefiltering, the gentler the transition. The effect that this prefilter has on the decoder step response is illustrated in Fig. 6b for four particular sampling clock phasings (in particular those phasings given by $t = 0$, $T/4$, $T/2$, and $3/T4$ on the time scale of Fig. 6a). As opposed to the no prefilter case where the step functions are simply delayed in time (see Fig. 4b), the addition of the prefilter results in an overlapping of the decoder step responses. After these decoder outputs are passed through the receiver rolloff filter,* the sharp corners will be smoothed and the width of the step response envelope will be reduced from the no prefilter case, as can be seen by comparing Fig. 6c with Fig. 4c. Thus sampling-induced busyness can be reduced at the expense of degraded rise times. The exact tradeoff between sampling-induced busyness (SIB) and average rise time (T_R) is given in Fig. 7 for a Gaussian-

* See the Appendix for an outline of the computer program used to derive system step responses for any combination of transition step size, prefilter step response, sampling rate, and quantizer.

shaped prefilter. The subjective weighting between these two factors is dependent upon picture content and will be discussed in Section IV after the quantizer effects are added.

The curve of Fig. 7 corresponds to a fixed sampling rate. Higher sampling rates will shift the curve closer to the analog case, and lower sampling rates will shift the curve further away from the analog case. This effect is illustrated in Fig. 8 for no prefiltering and for a Gaussian prefilter 6 dB down at 1 MHz. The higher the sampling rate, the closer the knee of the tradeoff curve approaches the analog condition of no busyness and a 0.69-μs rise time. Other families of prefilter shapes (non-Gaussian) produce slightly different SIB-T_R curves, but all exhibit the same tradeoff, reducing one only at the expense of increasing the other.

At this point it is necessary to discuss the validity of modeling the output of the *Picturephone* camera system as an ideal step function. The camera frequency characteristic is nominally flat to 1 MHz; therefore, as explained in Section II, the optics-to-optics step response is governed by the rolloff filter that is 20 dB down at 1 MHz and the ideal step function is a good model for the analog system. Since there

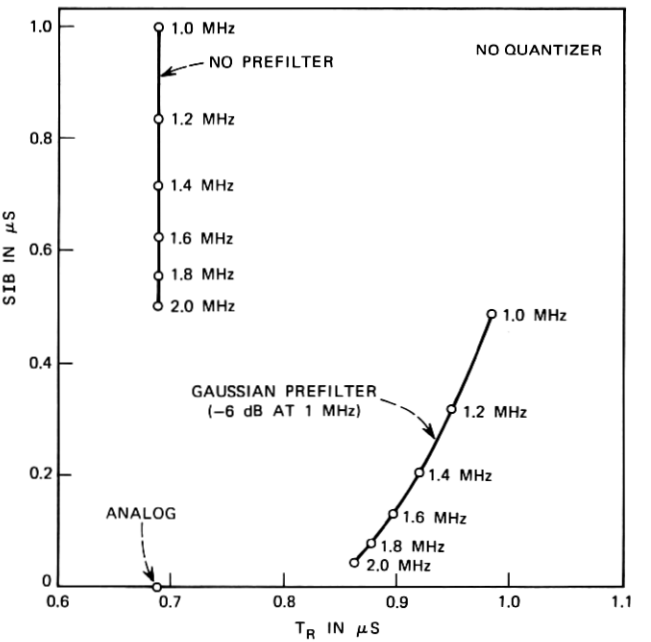

Fig. 8—SIB vs T_R for different sampling rates.

is a filter in the front end of the codec, the step-function model is also appropriate for the digital case as long as the frequency characteristic of the prefilter dominates that of the camera system. All prefiltering that will be seriously studied will be from 6 to 40 dB down at 1 MHz and will indeed dominate the camera system. In some instances, results will be given for less prefiltering (as in the case of points 0 and 0.1 in Fig. 7) and then it should be realized that these are somewhat idealized cases used only for illustrative purposes.

3.3 *Quantizer*

The addition of the quantizer-decoder combination completes the digital system given in Fig. 3. The quantizer is required in order to transmit over a finite digital channel. This necessary addition further confuses the edge indeterminacy—rise time picture given by the prefiltering and sampling circuits. The quantizer both produces its own edge indeterminance and affects average rise times. To see how a quantizer can produce edge indeterminance, refer to Fig. 9a. Here the step response of the prefilter is given by a smooth straight line. The quantizer used in this example has the standard Phase 0, companded DPCM 3-bit characteristic described in Ref. 3. With the sampling instants given at the bottom of Fig. 9a, the prefilter output could be coded as either decoder output No. 1 or No. 2, depending on slight noise variations at the beginning of the step. After passing through the receiver rolloff filter, the response to decoder outputs No. 1 and No. 2 is given in Fig. 9b by rolloff filter outputs No. 1 and No. 2 respectively. The

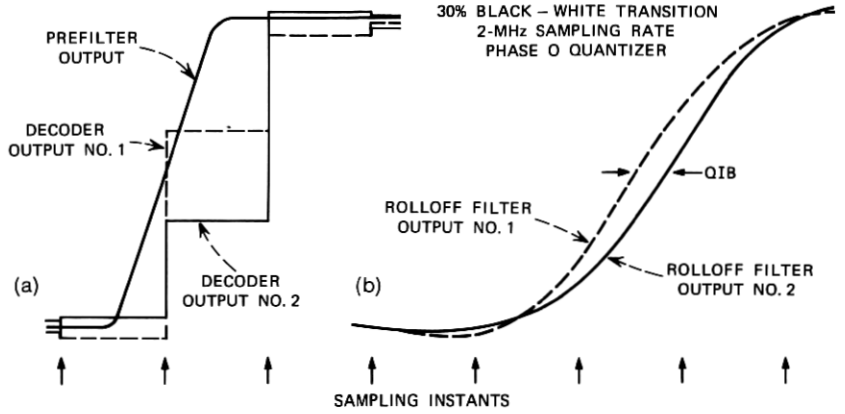

Fig. 9—Quantizer-induced busyness. (a) Prefilter and decoder outputs. (b) Resulting rolloff filter outputs.

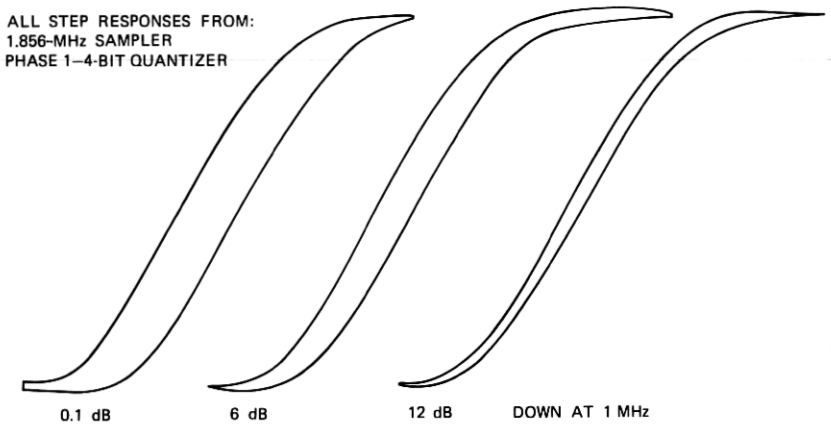

Fig. 10—Step response envelopes.

resulting edge indeterminance (again measured at the 50-percent amplitude point) is due to the quantizer and will henceforth be called quantizer-induced busyness (QIB). This quantizer-induced busyness is any resulting edge indeterminance over and above that which would be produced by just the prefiltering and sampling circuits. The total edge indeterminance resulting from a combination of both sampling- and quantizer-induced busyness will be referred to as edge busyness (EB). In all cases the edge busyness effect is calculated by varying the phase of the sampler. This phase difference can result in practice in many ways. It occurs spatially for a slanted line. It can result from a moving scene, from an unsynchronized codec, or from the residual phase jitter in a synchronized codec. It can also be shown that to some extent random noise on the video signal can be mapped into an equivalent sampling phase jitter.

The envelopes of possible step responses at the output of the receiver rolloff filter for the Phase 1 system are given in Fig. 10 for a Gaussian prefilter that is 0.1, 6, and 12 dB down at 1 MHz (see the Appendix for calculations). This Phase 1 system employs a 1.856-MHz sampler and a companded DPCM 4-bit quantizer which is described in detail in Table I. Again the prefilter yields a tradeoff between edge busyness and rise time. For any combination of sampling rate and quantizer, the prefilter yields this same type of tradeoff. To assign numbers to this characteristic, Fig. 11 plots edge busyness versus rise time for the Phase 1 system with varying amounts of Gaussian prefiltering. Also plotted for comparison purposes is the sampling-induced busyness—rise time tradeoff already given in Fig. 7.

TABLE I—PHASE 1, 4-BIT QUANTIZER CHARACTERISTIC

Output Level Number	Quantized Signal Output* $\left(\frac{\text{weight}}{128}\right)$
1, 2	± 1
3, 4	± 3
5, 6	± 7
7, 8	±15
9, 10	±23
11, 12	±31
13, 14	±39
15, 16	±47

* Weights are relative to the smallest quantum step of a 7-bit PCM system. See Ref. 4 for additional information.

The addition of the quantizer complicates the problem even more than already discussed. Up to this section the results have been independent of the magnitude of the black-white transition. Fig. 11 results from using a 40-percent black-white transition with the Phase 1 4-bit

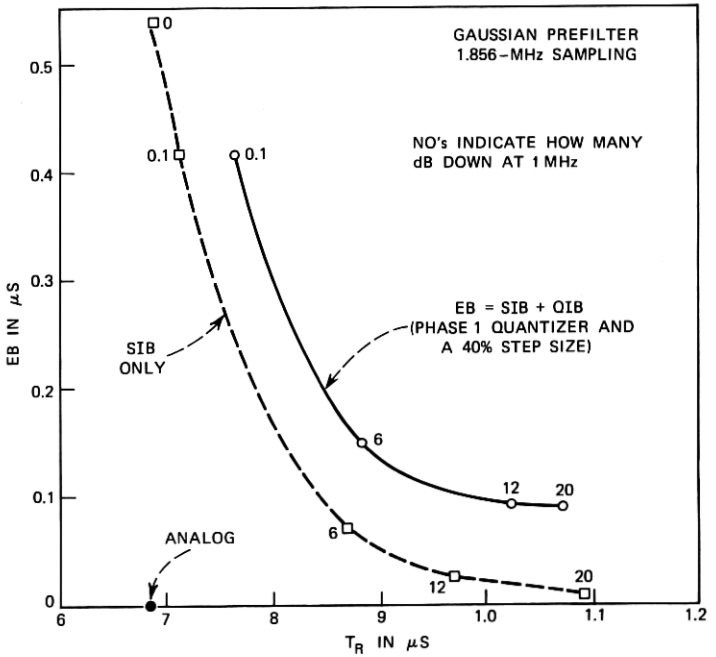

Fig. 11—Edge busyness—rise time tradeoffs.

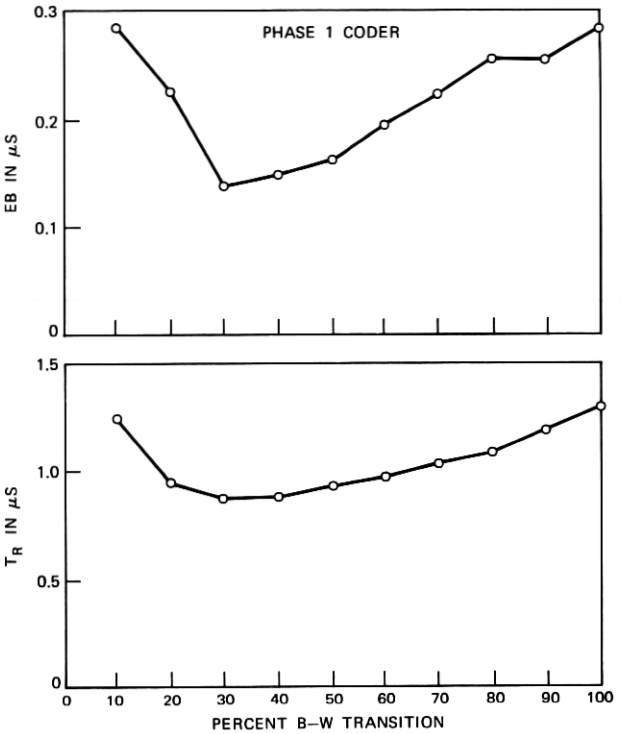

Fig. 12—Edge busyness and rise time vs step size.

quantizer. Both edge busyness and rise time are plotted versus step size in Fig. 12 for the Phase 1 coder using its 6-dB Gaussian prefilter. The shape of both curves can be explained using Fig. 13, where both the quantizing noise and the step-size-to-quantizing-noise ratio are plotted versus step size. Both edge busyness and rise time are inversely proportional to the signal-to-noise ratio and are therefore minimized at a step size of 30 to 40 percent where the signal-to-noise ratio is maximized. For the remainder of this study only three measures of system quality will be considered. These three measures are:

(*i*) the edge busyness and rise time of the 40-percent step size (M4),

(*ii*) the average edge busyness and average rise time for the 10, 20, 30, and 40 percent step sizes (M1-4),

(*iii*) the average edge busyness and average rise time for the 10 step sizes from 10 to 100 percent (M1-10).

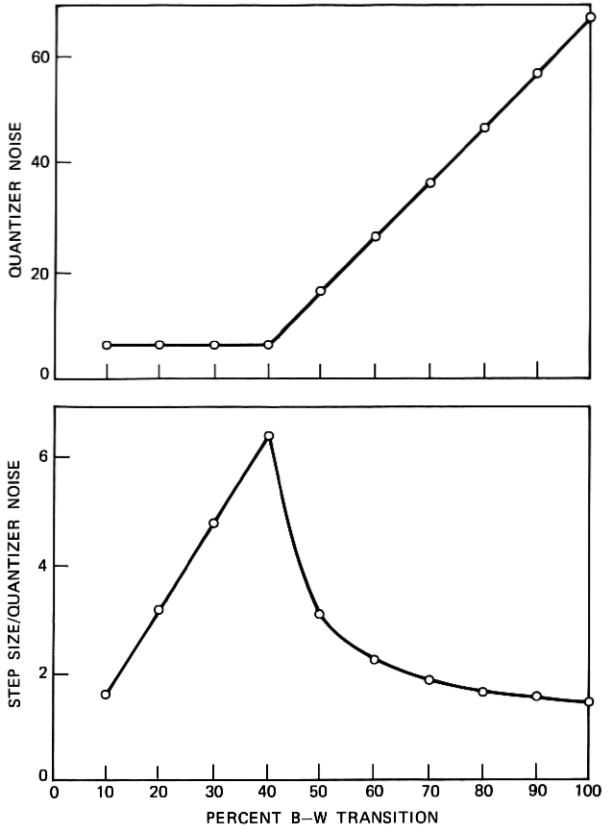

Fig. 13—Quantizer noise and SNR vs step size.

Measure M4 has the advantage of simplicity. Edge busyness can easily be seen on a transition of this size. This is also the breakpoint shown in Fig. 13 before the quantizer's slope overload characteristic takes effect. Measure M1-4 averages over the lower four step sizes. Typically 95 to 99 percent of all transitions are below a 40-percent step size for a 2-MHz sampler. Measure M1-10 uses the most information and disregards all assumed knowledge of observer subjective effects. All three measures were used in designing the coders that will be discussed in the following sections. Ultimate justification for these measures rests with the subjective evaluation of coders with quantizers as will be discussed in Section VI.

IV. SUBJECTIVE EVALUATION OF THE EDGE BUSYNESS—RISE TIME TRADEOFF

In the last section it was shown how the variation of the prefilter yielded a tradeoff between edge busyness and average rise time for any combination of sampling rate and quantizer structure. In this section a series of subjective tests will be described that were run to find the subjectively optimum edge busyness—rise time tradeoff. For these tests only sample-and-hold circuits were used in order to avoid the question of which measure to use when quantizers are involved. In Section VI a series of subjective tests will be described using coders with quantizers.

The test consisted of asking each of 30 observers to rate various systems on the basis of three different source pictures. The first camera source was a mannequin, set up as shown in Fig. 14. This mannequin,

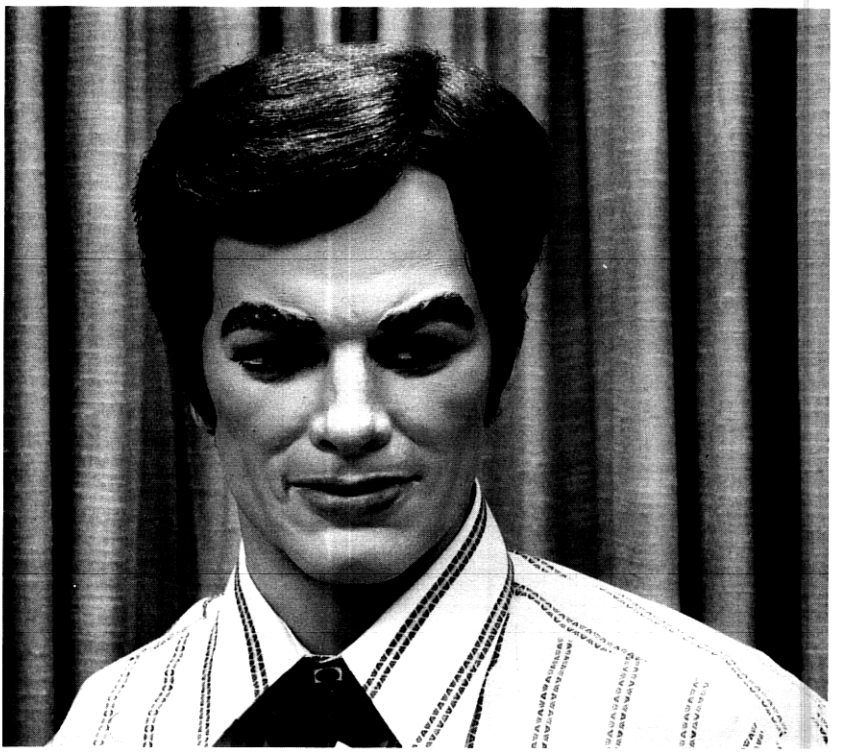

Fig. 14—Microhenry.

"Microhenry" or "Mike" for short, is mounted on a platform which tilts him in a symmetric, sinusoidal fashion from side to side. He is pivoted approximately 14 inches below his chin and was moved a maximum of ± 13 degrees from the vertical at a rate of one cycle every 4.3 seconds. The second and third camera sources were slides of Karen and a graph, as shown in Figs. 15 and 16, respectively. Both of these sources were stationary. For all three sources, each of the 30 observers was given an AB type test wherein the observer was presented with 36 different pairs of systems and asked to pick the most pleasing or the most readable of each pair (most pleasing for each test given on Mike and Karen and most readable for those tests given on the graph). These 36 pairs include all meaningful comparisons between nine different systems. If the pair (A, B) = (system 6, system 9) was given, then pair (A, B) = (system 9, system 6) would not be included. Similarly there was no AB of any system with itself. Each of these nine systems consisted only of a prefilter followed by a sample-and-hold circuit. All prefilters had a crispened Gaussian amplitude characteristic which, along

Fig. 15—Karen.

with near-linear phase, resulted in a symmetric step response with single 4-percent undershoot and overshoot. Five different prefilters were used, being designed to be 3, 6, 10, 20, and 40 dB down at 1 MHz. After tuning, these filters were measured to be 3.0, 5.4, 9.6, 18.4, and 38.1 dB down at 1 MHz with approximately linear phase. The sample-and-hold circuit was driven by one of three sampling clocks, each of which was synchronized to the camera video. The three sampling clocks had synchronized frequencies of 2.015, 1.512, and 1.200 MHz. The particular numbering sequence with system characteristics is listed in Table II. Both the predicted and the measured performance characteristics of these nine systems, as specified on an edge busyness—rise time chart, are given in Fig. 17. Each test was given using an unmodified Mod 2C *Picturephone* station set as the receiver, with the observer given complete freedom of its brightness control. Processing the resulting data for each camera source using standard-pair comparison techniques[5] results in the scale values plotted in Fig. 18. These scale values are a psychological measure of relative coder preference; the higher the scale value, the more the coder is preferred. The least

Dhro S 60¢ ennto! A "moa" r

SITNENU 93% ECST-HIHE FS/SG

Rhl, V363 eoalm $17,462 mivuen pe ng Votre Chaı

Sa (Rti) foalt ? 0.37 + 4.2 = - 3/4 ? Eht eplue .37+4.

N. Y. atf tee CB&M.H.T. Op472rf.Tsr atn nuf SSF eh

"RE tzwhto", won $247.17 frf ufeud ono Fun Rmt Assf ehih "aou

(Saeli) oh nef:she 3/4 rnm&sr "af "aebo", lw Ypr 17% neu

Ihpp asl ! ($71.366 + 17¢) oon ifa neonelyf I6st HL ½ Fylenoen 17856 Un

Fig. 16—Graph.

TABLE II—SYSTEM CHARACTERISTICS

System Number	Sampling Rate	Prefilter*
1	2.015 MHz	6
2	1.512 MHz	3
3	1.512 MHz	10
4	1.512 MHz	20
5	1.512 MHz	40
6	1.200 MHz	3
7	1.200 MHz	10
8	1.200 MHz	20
9	1.200 MHz	40

* Specified by the number of dB down at 1 MHz.

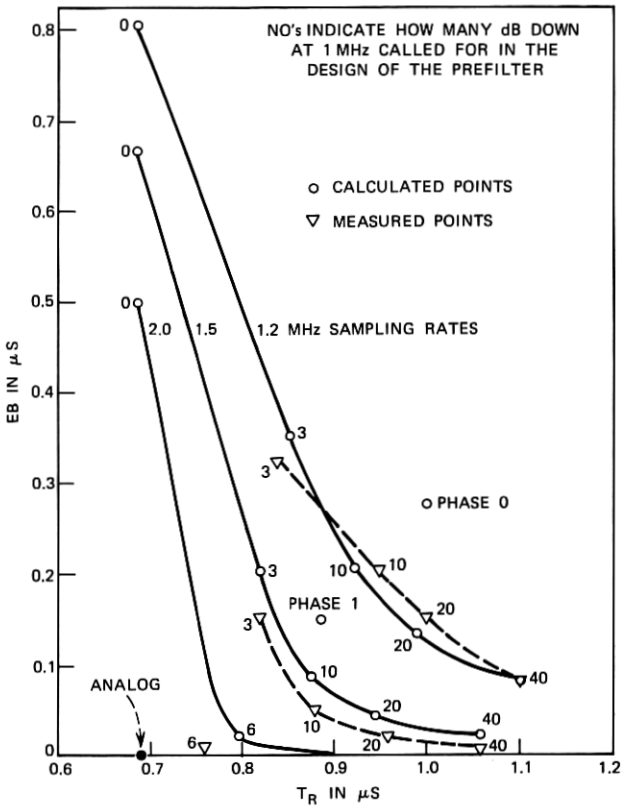

Fig. 17—Edge busyness—rise time tradeoffs for subjective tests.

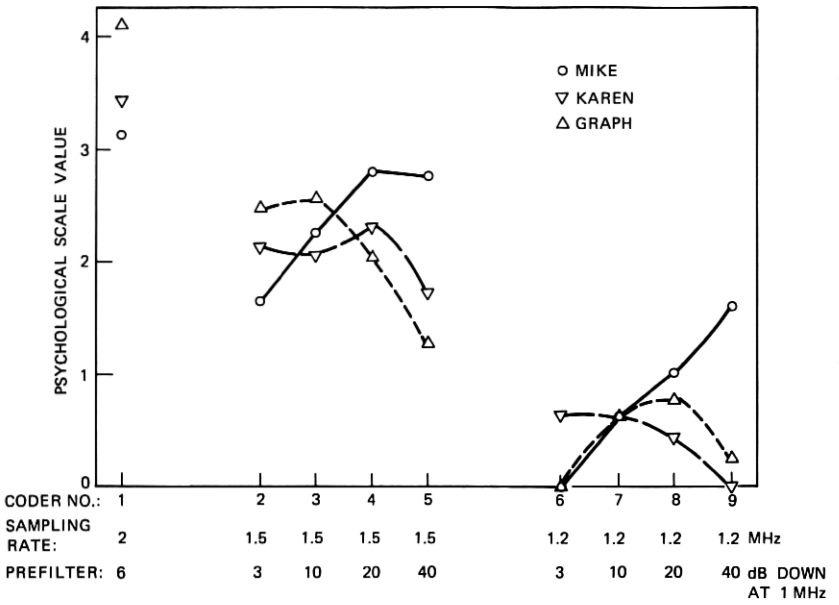

Fig. 18—Psychological scale values for Mike, Karen, and graph.

preferred coder is arbitrarily assigned the value zero with all other coders scaled relative to the worst. The following properties should be noted:

(*i*) No intersource numerical comparisons should be made. A scale value of 4.13 for the best graphics coder and 3.13 for the best coder on Mike only means that the observers were more discriminating on the graphics source. It does not mean that the best graphics coding is better than the best coding of Mike.

(*ii*) Mike is somewhat of a worst case for aliasing. His shirt was chosen for its narrow stripes because undersampling is most harmful when appreciable high-frequency content is present. This undersampling causes the straight edges to appear crooked and the moving subject imparts a distinctive motion to them. On Mike most observers found aliasing to be the only degradation caused by the different systems and hence the narrower prefilters were preferred because they yielded less aliasing at the expense of lower picture resolution. A prefilter that is 20 dB down at 1 MHz was preferred for the 1.5-MHz sampling

rate and a prefilter 40 dB down was preferred for the 1.2-MHz system.

(*iii*) Karen has been a much-used source where both edge busyness and resolution are important. The aliasing still shows up as crooked stripes in her blouse, but they are motionless for our synchronized clocks and therefore not quite as annoying. For this source a 20-dB prefilter was preferred for the 1.5-MHz system and a 3-dB prefilter was preferred for the 1.2-MHz system.

(*iv*) The graph's sole property is readability. Here the 10-dB prefilter was preferred for the 1.5-MHz system and the 20-dB prefilter was preferred for the 1.2-MHz system.

Since Mike is a worst case for aliasing, Karen a difficult source for both aliasing and resolution, and the graph a test of readability, the three sources are considered to be of equal importance, and all 90 responses will be lumped together for the final preference scale. Analyzing these 90 responses by the pair comparison analysis[5] results in the scale values shown in Fig. 19. The 2-MHz system is preferred over the best 1.5-MHz system which is in turn preferred over the best 1.2-MHz system. There is a fairly broad range of optimum prefiltering for the 1.5-MHz system with the best prefilter 20 dB down at 1 MHz. For the 1.2-MHz system, the narrower the prefilter the better, with the best choice of those studied being 40 dB down at 1 MHz.

As shown in Fig. 17, these results indicate that the best subjective tradeoff between edge busyness and rise time occurs just below the knee

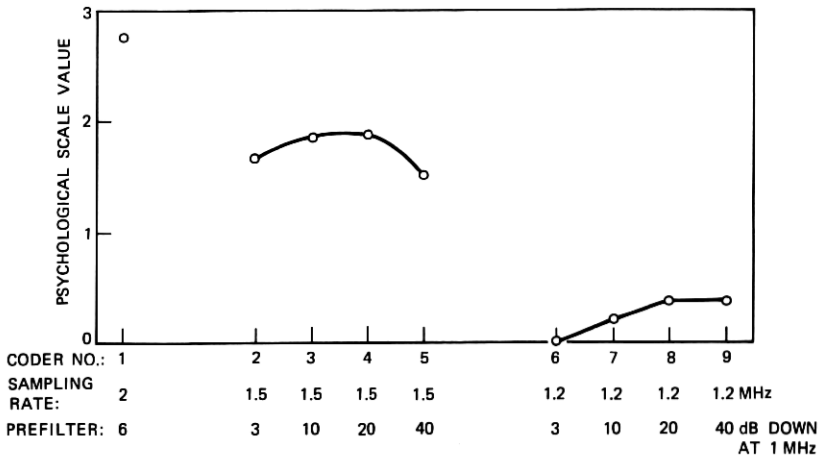

Fig. 19—Psychological scale values resulting from all 90 responses.

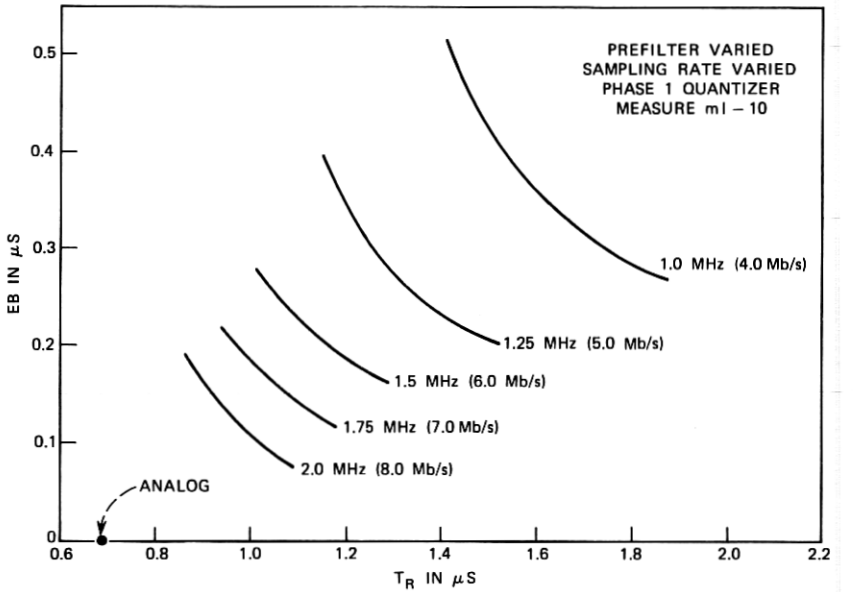

Fig. 20—Edge busyness—rise time tradeoffs for the Phase 1 quantizer.

of each tradeoff curve where the incremental reduction in edge busyness becomes small compared to the incremental increase in average rise time.

V. OPTIMIZING THE SAMPLING RATE FOR A FIXED TRANSMISSION RATE

For the Phase 1 4-bit companded DPCM quantizer given in Table I, the variation of both prefilter and sampling rate leads to the tradeoffs between edge busyness and average rise time given in Fig. 20. These curves are not unexpected; for any combination of sampling rate and quantizer, the prefilter leads to a tradeoff between edge busyness and average rise time. The higher the sampling rate (and therefore the higher the transmission rate in this case), the closer the knee of the tradeoff curve approaches the analog case and therefore the better the picture quality. Figure 20 results from using a crispened Gaussian prefilter. Many other filter shapes were studied in an attempt to find the best edge busyness—rise time tradeoff curves. At the higher sampling rates (namely 1.856 MHz and above) the prefilter shape becomes unimportant; here, less prefiltering is required and the receiver rolloff filter becomes increasingly dominant. As the sampling rate is

reduced, two things are desired in filter shaping: rapid amplitude falloff versus frequency and controlled overshoot in the time domain. The rapid falloff is required to control aliasing without removing significant video information and controlled overshoot is needed to present a pleasing picture, one without excessive ringing. The crispened Gaussian filter shape with 4-percent overshoots, as specified by eq. (1) with $K = 0.5292$ but with T a variable, yields a good compromise between these two factors.

The results given in Fig. 20 show the effects of different sampling rates with a single quantizer. The transmission rate is proportional to the sampling rate and the number of bits used to code each sample. Therefore, in the extreme case, we are comparing the performance of an 8-Mb/s transmission system (2-MHz sampler–4-bit quantizer) with that of a 4-Mb/s transmission system (1-MHz sampler–4-bit quantizer). The more interesting tradeoff results from considering a specific transmission rate. For any given transmission rate, what is the best combination of prefilter, sampling rate, and quantizer which minimizes both edge busyness and average rise time? A higher sampling rate implies fewer quantizing levels which means less SIB but more QIB. A lower sampling rate implies more quantizing levels which means more SIB but less QIB. The prefilter is used to trade off edge busyness against picture resolution to yield the best subjective picture quality for each sampling rate–quantizer combination.

To be specific, given the following three transmission rates*

(*i*) 6. Mb/s
(*ii*) 7.5 Mb/s
(*iii*) 8. – 9. Mb/s

what is the optimum combination of sampling rate and number of bits/sample?

For the 6.-Mb/s rate, the first three coders listed in Table III are considered. In order to simplify the calculations, only the first performance measure, M4, slightly modified, is calculated. A 40-percent video transition is used with the 2.0-MHz system, a 50-percent transition with the 1.5-MHz system, and a 60-percent transition with the

* The 6.-Mb/s rate results from the simplest use of a T2 line. The effective bit rate of 7.5 Mb/s results from using 300 cells of storage to expand video information into the horizontal sync pulse interval with subsequent transmission over a T2 line. An effective bit rate of 8 to 9 Mb/s can be achieved over a T2 line by using about 20,000 cells of storage (see Ref. 6) to use both the horizontal sync pulse interval and variable length coding. This variable length coding takes advantage of the statistical properties of the video signal.

TABLE III—CODER CHARACTERISTICS

Transmission Rate	Sampling Rate	Quantizer
6.0 Mb/s	2.0 MHz	3-bit DPCM
6.0 Mb/s	1.5 MHz	4-bit DPCM
6.0 Mb/s	1.2 MHz	5-bit DPCM
7.5 Mb/s	1.9 MHz	4-bit DPCM
7.5 Mb/s	1.5 MHz	5-bit DPCM
7.5 Mb/s	1.2 MHz	6-bit DPCM
8.3 Mb/s	1.9 MHz	5-bit DPCM
9.0 Mb/s	1.5 MHz	6-bit DPCM
8.4 Mb/s	1.2 MHz	7-bit DPCM

1.2-MHz system. This modification accounts for the longer sampling intervals encountered with the lower sampling rates. For each coder a wide range of prefilters was evaluated and the optimum prefilter chosen using the subjective results given in Section IV. The prefilter which results in an edge busyness—rise time tradeoff just below the knee of the curve was chosen. The three resulting systems are given by the upper curve of Fig. 21. For the effective bit rate of 7.5 Mb/s, the middle three coders listed in Table III are considered. Using similar optimization procedures, these three coders result in the three edge busyness—rise time points given by the middle curve of Fig. 21. For the 8. to 9.-Mb/s transmission rate, it is assumed that variable length coding will result in an extra bit per sample for each of the sampling rates used. Here the three coders listed in the bottom of Table III are

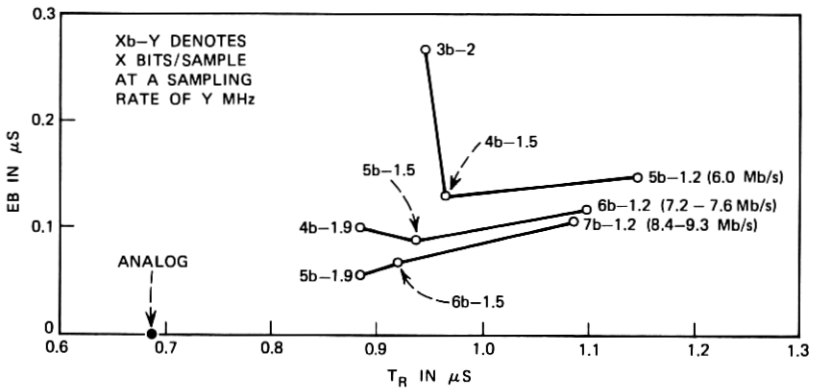

Fig. 21—Edge busyness—rise time tradeoffs for fixed transmission rates.

considered. These coders result in the three edge busyness—rise time points given by the lower curve of Fig. 21.

Examination of Fig. 21 leads to the following conclusions:

(*i*) For intraframe coders operating at an effective bit rate of 6 Mb/s (points 3b-2., 4b-1.5, and 5b-1.2 on Fig. 21), the edge busyness—rise time tradeoff is optimized by using a 1.5-MHz sampling rate and a 4-bit quantizer coupled with a *Picturephone*-type prefilter 20 dB down at 1 MHz.

(*ii*) For intraframe coders operating at an effective bit rate of 7.5 Mb/s (points 4b-1.9, 5b-1.5, and 6b-1.2), the edge busyness—rise time tradeoff is optimized by using a sampling rate of either 1.5 or 1.9 MHz, with no significant advantage associated with either of the two sampling rates.

(*iii*) Only after an intraframe coder is operating at a bit rate higher than 7.5 Mb/s (points 5b-1.9, 6b-1.5, and 7b-1.2) does it become beneficial to sample at 2 MHz.

VI. SUBJECTIVE EVALUATION OF *PICTUREPHONE* CODERS

The main point indicated in Section V was that the optimum sampling rate is some function of the transmission rate. This point is most dramatically illustrated for a transmission rate of 6. Mb/s. Here it is predicted that a 4-bit–1.5-MHz coder will outperform the Phase 0 coder (3-bit–2.0-MHz). In order to check this point subjectively, the same 30 observers used in Section IV were given an AB test between the Phase 0 coder and a coder consisting of a crispened Gaussian prefilter 20 dB down at 1 MHz, a synchronized 1.512-MHz sampling clock, and the Phase 1 4-bit quantizer. Each observer was asked to pick the most pleasing coder for Mike and Karen and the most readable coder for the graph. A summary of the results for the Phase 0–4-bit–1.5-MHz AB comparison is given below:

	Prefer Phase 0	Prefer 4-bit–1.5-MHz
Mike:	22	8
Karen:	3	27
Graph:	7	23
All:	32	58

Overall, the 4-bit–1.5-MHz coder was preferred over Phase 0 by a margin of nearly 2:1, giving some justification for the two-factor tradeoff analysis.

In order to find out where the edge busyness—rise time impairments lie on an absolute quality scale, a series of unimpaired-impaired type comparisons were used to rate six different coders on a five-comment impairment scale. For each of the three camera sources, each observer made a comparison of all six coders to the unimpaired analog video signal and was asked if the impairment added by the coder was:

(*i*) not noticeable (weight = 1)
(*ii*) just noticeable (weight = 2)
(*iii*) noticeable but not objectionable (weight = 3)
(*iv*) objectionable (weight = 4)
(*v*) extremely objectionable (weight = 5).

Six different coders were evaluated; these were:

(*i*) Phase 1 (1.856-MHz, 4-bit DPCM, 6-dB Gaussian prefilter)
(*ii*) Phase 0 (2.0-MHz, 3-bit DPCM, 6-dB Gaussian prefilter)
(*iii*) the 4-bit–1.5-MHz coder used in the previous AB comparison with Phase 0
(*iv*) a 2.0-MHz sample-and-hold system using a 6-dB crispened Gaussian prefilter (System 1 of Section IV)
(*v*) a 1.5-MHz sample-and-hold system using a 20-dB crispened Gaussian prefilter (System 4 of Section IV)
(*vi*) a 1.2-MHz sample-and-hold system using a 40-dB crispened Gaussian prefilter (System 9 of Section IV).

The detailed results of the comment scale ratings in terms of means and standard deviations for Mike, Karen, the graph, and all of the responses are listed in Table IV. When all 90 responses are lumped together, the six coder means are given below (see the next to the last row of Table IV).

	Mean Comment Scale Rating
2.0-MHz sample-and-hold:	1.63
1.5-MHz sample-and-hold:	2.12
1.2-MHz sample-and-hold:	3.46
Phase 1:	2.59
Phase 0:	3.31
4-bit–1.5-MHz:	3.30

Here a lower mean comment scale rating is preferable, indicating a lower amount of impairment added by the coder. Note that although

TABLE IV—COMMENT SCALE RESULTS

Coder: Prefilter: Samp. Rate: Quantizer:	4b-1.5 20 1.5 4	Phase 0 6 2.0 3	Phase 1 6 1.9 4	2.0 S&H 6 2.0 —	1.5 S&H 20 1.5 —	1.2 S&H 40 dB 1.2 MHz — Bits
Mike Mean:	3.27	2.85	2.50	1.78	2.10	3.05
Standard Deviation:	0.96	0.78	0.86	0.79	0.61	0.78
Karen Mean:	3.23	3.38	2.48	1.28	1.60	3.32
Standard Deviation:	0.63	0.54	0.72	0.50	0.65	0.89
Graph Mean:	3.40	3.68	2.80	1.82	2.67	4.00
Standard Deviation:	0.85	0.66	0.88	0.76	1.06	0.96
All 90 Responses Mean:	3.30	3.31	2.59	1.63	2.12	3.46
Standard Deviation:	0.83	0.75	0.84	0.74	0.91	0.97

on an AB test the 4-bit–1.5-MHz coder was chosen over the Phase 0 coder by a margin of almost 2:1, when placed on a quality scale and separated in time, they are rated as being equal. In using these ratings it should be remembered that the three camera sources were picked to give all intraframe coders trouble. If Mike did not have a striped shirt or Karen a striped blouse, these tests would have shown very little difference between the coders and all would have been rated much more leniently.

In Fig. 22, the six coders used in the above subjective tests are plotted on an edge busyness—rise time chart. A 40-percent step size is used for both the Phase 0 and Phase 1 coders while a 50-percent step size is used for the 4-bit–1.5-MHz coder. All sample-and-hold coder coordinates are independent of the step size due to lack of a quantizer. With the mean scale values indicated in parentheses, it becomes apparent that the general edge busyness—rise time analysis is further substantiated. The closer the coordinates to the analog case the better, with almost equal weighting between the edge busyness and rise time axes, edge busyness being slightly more undesired than reduced rise time. (See Section IV where points just under the knee of each curve were chosen.) The two dashed circles with centers on the analog coordinates approximate equal-impairment contours with the

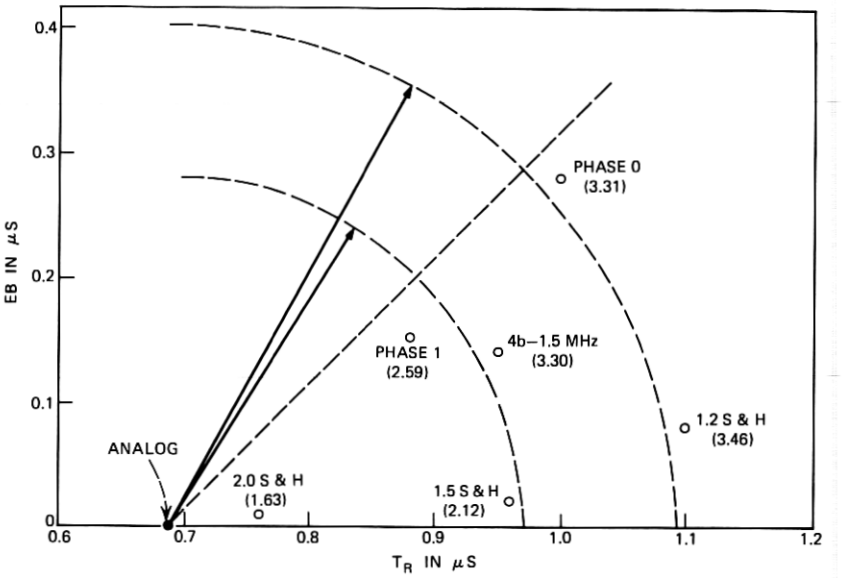

Fig. 22—Comment scale values as a function of edge busyness and rise time.

dashed 45-degree line giving equal weighting to both edge busyness and increased average rise time.

Finally it is noted that only station sets using crispened Gaussian postfilters which are 20 dB down at 1 MHz have been assumed. Other postfilters were tried, including some in the Butterworth family, and similar results were obtained. Any postfilter which affects the analog system to only a minor degree is not expected to significantly change the results presented in this paper.

VII. SUMMARY

A description of the two main degradations inherent in present intraframe video coders has been presented. Methods allowing a tradeoff between these two degradations, edge busyness and reduced rise time, have been described; and optimum coder composition, including prefiltering, sampling rate, and quantizer structure, has been presented as a function of transmission rate. A subjective testing program has been carried out which substantiates the edge busyness—rise time evaluation of video coders and rates a number of intraframe coders on a five-comment impairment scale.

APPENDIX

Edge Busyness—Rise Time Program

Program Inputs: (*i*) Step Size $[A]$
(*ii*) Prefilter Step Response $[b(t)]$
(*iii*) Sampling Rate $[f_s = 1/T]$
(*iv*) Quantizer Structure.

Program Computations:

A.1 *For each of 20 uniform phasings:*

$$(\phi_i, i = 1, 20) = (i - 1)T/20. \tag{3}$$

A.1.1 Determine a series of sample-and-hold values for the system as given in Fig. 3.

$$(X_{ij}, j = 1, 10) = (Ab[\phi_i + T(j - 1)]). \tag{4}$$

A.1.2 Transform sample-and-hold series from A.1.1 into a series of values that would be transmitted over the digital channel.

$$Y_{i1} = Q(X_{i1}) \tag{5}$$

$$(Y_{ij}, j = 2, 10) = \left(Q\left[X_{ij} - \sum_{k=1}^{j-1} Y_{ik}\right]\right) \tag{6}$$

where $Q(a)$ refers to the quantized value of a that can be calculated using the quantizer structure. All thresholds are located midway between the output levels.

A.1.3 Digitally add the quantized series from A.1.2 as would be done by the decoder to result in the quantized version of the sample-and-hold values of A.1.1.

$$(Z_{ij}, j = 1, 10) = \left(\sum_{k=1}^{j} Y_{ik}\right). \tag{7}$$

A.1.4 Since the series produced in A.1.3 represents the amplitude of a series of rectangular pulses approximating the original input video signal, summing a series of appropriately amplified and delayed *Picturephone* receiver step responses as given by eq. (2) of the text will result in the video output of the *Picturephone* station set.

$$Z(t) = \sum_{k=1}^{10} Y_{ik} s[t - \phi_i - (k - 1)T]. \tag{8}$$

A.1.5 Use a search procedure on this video output to find the instants of time when the waveform is equal to 10, 50, and 90 percent of the input step amplitude.

A.2.1 Calculate the output

$$T_R = \frac{1}{20} \sum_{i=1}^{20} (T_{i90} - T_{i10}) \tag{9}$$

as the average 10- to 90-percent rise time.

A.2.2 Calculate and output

$$EB = \max_i (T_{i50}) - \min_i (T_{i50}) \tag{10}$$

as the edge busyness measure.

The above procedure can be used to calculate the combined effects of SIB and QIB or the effect of SIB only, since replacing the quantizer with an identity equation leaves only the effects of SIB to be calculated. It is not possible to calculate the effects of QIB only, since presampling is required for the quantizer.

For all plots given in this paper, eq. (8) can be placed inside a DO loop to calculate the output waveform for a wide range of times.

REFERENCES

1. Cagle, W. B., Stokes, R. R., and Wright, B. A., "The *Picturephone*® System: 2C Video Telephone Station Set," B.S.T.J., *50*, No. 2 (February 1971), pp. 271–312.
2. Crater, T. V., "The *Picturephone*® System: Service Standards," B.S.T.J., *50*, No. 2 (February 1971), pp. 235–269.
3. Millard, J. B., and Maunsell, H. I. G., "The *Picturephone*® System: Digital Encoding of the Video System," B.S.T.J., *50*, No. 2 (February 1971), pp. 459–479.
4. Abbott, R. P., "A Differential Pulse-Code-Modulation Coder for Videotelephony Using Four Bits Per Sample," I.E.E.E. Trans. Commun. Tech., *COM-19*, No. 6, Part 1 (December 1971), pp. 907–912.
5. Edwards, A. L., *Techniques of Attitude Scale Construction*, New York: Appleton-Century-Crofts, Inc., 1957, pp. 40–46.
6. Chow, M.-C., "Variable-Length Redundancy Removal Coders for Differentially Coded Video Telephone Signals," I.E.E.E. Trans. Commun. Tech., *COM-19*, No. 6, Part 1 (December 1971), pp. 923–926.